

1 **Research Article**

2 **A Novel Grape Downy Mildew Resistance Locus**
3 **from *Vitis rupestris***

4 Gaurab Bhattarai,¹ Anne Fennell,² Jason P. Londo,³ Courtney Coleman,¹ and
5 Laszlo G. Kovacs^{1*}

6 ¹Department of Biology, Missouri State University, Springfield, MO 65897; ²Department of
7 Agronomy, Horticulture & Plant Science, South Dakota State University, Brookings, SD
8 57007; and ³Grape Genetics Research Unit, USDA-Agriculture Research Service, Geneva,
9 NY 14456.

10 *Corresponding author (Laszlokovacs@missouristate.edu; tel: 417-429-3862)

11 Acknowledgments: The authors thank John Heywood, Zoë Migicovsky, Avinash Karn,
12 Allison Miller, Laura Klein, Daniel Wilkinson, Sonu Koirala BK, and Mani Awale for their
13 help with various aspects of this work. This work was supported by funds from the National
14 Science Foundation Plant Genome Research Program (Award No. 1546869), the USDA-
15 NIFA Specialty Crop Research Initiative (Award No. 2011-51181-30635), the South Dakota
16 Agricultural Experiment Station, Hatch Project No. SD00H633-18, and the Missouri State
17 University Graduate College.

18 Manuscript submitted May 9, 2020, revised Aug 5, 2020, accepted Aug 10, 2020

19 Copyright © 2020 by the American Society for Enology and Viticulture. All rights reserved.

20 By downloading and/or receiving this article, you agree to the Disclaimer of Warranties and
21 Liability. The full statement of the Disclaimers is available at
22 <http://www.ajevonline.org/content/proprietary-rights-notice-ajev-online>. If you do not agree
23 to the Disclaimers, do not download and/or accept this article.

24
25 **Abstract:** The viticulture industry needs advanced grape cultivars encoding genetic
26 information that enhances disease resistance and environmental stress tolerance to meet the
27 challenges of a changing climate. To discover beneficial allelic variants of grape genes, we
28 established an F₁ mapping population from a cross between two North American grapevines,
29 *Vitis rupestris* Scheele and *Vitis riparia* Michx. We generated genotyping-by-sequencing
30 (GBS) markers and constructed parental linkage maps consisting of 1,177 and 1,115 GBS
31 markers, respectively (LOD threshold ≥ 14), which were validated by mapping the sex-

32 determining locus to chromosome 2. Taking advantage of loci heterozygous in both parents,
33 we also constructed an integrated map containing 2,583 markers. We mapped a major QTL
34 for downy mildew (*Plasmopara viticola*) resistance to chromosome 10 of *V. rupestris* using
35 both greenhouse- and *in vitro*-generated leaf resistance data. This QTL explains 66.5% of the
36 phenotypic variance under greenhouse conditions, and its 2-LOD confidence interval
37 corresponds to region 2,470,297 to 3,024,940 bp on chromosome 10 in the *Vitis vinifera* L.
38 PN40024 reference genome sequence (assembly 12X.v2). We provide PN40024-projected
39 positions of the GBS markers, which can be used as anchors to develop additional markers
40 for the introgression of this *V. rupestris* haplotype into cultivated grape varieties.

41 **Key words:** disease resistance, linkage map, QTL, *Plasmopara viticola*, QTL, *Vitis riparia*,
42 *Vitis rupestris*

43 Introduction

44 Grape (*Vitis vinifera* L.) cultivation relies heavily on the recurrent application of
45 fungicides, a disease control method that is costly, and potentially harmful to the
46 environment and human health. Cultivation of disease-resistant grape varieties carrying
47 genes that enhance defense against pathogens is an approach that helps reduce the amount of
48 fungicides applied in viticulture. Traditionally, the source of such defense-related genes has
49 been the North American wild relatives of *V. vinifera*, as they have coevolved with now
50 pandemic pathogens and acquired allelic diversity that strengthens resistance against fungal
51 and oomycete diseases (Alleweldt and Possingham 1988). Grapevine breeding has a long
52 history of introgressing genetic information from wild grapevines (*Vitis* species) into *V.*
53 *vinifera*. The first interspecific grapevine crosses were made in the United States during the

54 early and mid-19th century, followed by a surge of breeding activity in Europe in the wake of
55 the phylloxera epidemic in the late 19th and early 20th centuries (Reisch et al. 2012). This
56 pioneering work focused on developing disease-resistant fruit-producing varieties through
57 crosses between *V. vinifera* and North American grape species, and breeding phylloxera- and
58 lime-tolerant rootstocks through interspecific crosses among various American grapevines.
59 These efforts met with great success, to the extent that hybrids from the late 19th century are
60 still popular fruit-producing varieties in the eastern and mid-western US, and that several of
61 the interspecific American hybrids are among the most widely used rootstocks worldwide
62 even today (Di Gaspero et al. 2012, Migicovsky et al. 2016, Riaz et al. 2019).

63 While the introgression of disease resistance traits continued through the 20th
64 century, the exploration of wild grape relatives for new resistance sources has lagged. Most
65 of the breeding work during the past century focused on germplasm that had been introduced
66 to Europe from North America during the 1800s. This resulted in a narrow genetic base for
67 both fruit-producing and rootstock hybrids as documented by Di Gaspero et al. (2012) and
68 Riaz et al. (2019), respectively. The high degree of polymorphism reported in North
69 American wild grapevines (Liang et al. 2019) suggests that the genetic diversity of this
70 germplasm is vastly more extensive than what is represented in hybrid cultivars today.
71 Recent examples in which a broader exploration of this germplasm led to the discovery and
72 deployment of valuable haplotypes include the introgression of Pierce's disease resistance
73 from *Vitis arizonica* (Riaz et al. 2009) and powdery and downy mildew resistance from
74 *Muscadinia rotundifolia* (Feechan et al. 2013, Agurto et al. 2017).

75

76 In this paper, we describe linkage map construction and QTL analysis in an F₁ family
77 from a cross between *V. rupestris* and *V. riparia*, two species that vary in habitat and in
78 adaptation to different environmental conditions. The seed parent used in this cross is *V.*
79 *rupestris* B38, which was collected by Herbert C. Barrett in Texas in 1951 and donated to the
80 National Germplasm Repository in Geneva, NY (PI588160) by Bruce Reisch in 1985. The
81 pollen parent is *V. riparia* HP-1, which was collected by Neils E. Hansen in Bismarck, ND
82 and donated to the National Germplasm Repository in Geneva, NY (PI588271) by Ronald
83 Peterson in 1987. *V. rupestris* forms shrubs that sprawl along the surface of nutrient-poor
84 sand or gravel bars in intermittent streams or stony outcroppings, and grows in small
85 populations within a limited geographic area. *V. riparia*, a sister taxon of *V. rupestris*, forms
86 high-climbing lianas in moist but well-drained alluvial soils along rivers, and thrives in large
87 populations across great expanses of the continent. As these evolutionary closely related
88 grapevine species (Klein et al. 2018), have adapted to contrasting environmental conditions
89 in their native habitats, their alleles will likely influence horticultural traits in different
90 ways. The parent plants were selected because they have large differences in fall photoperiod
91 response, which is likely tied to cold tolerance, and because we wanted to pseudo-replicate
92 the specific cross that had produced the commercial rootstock 3309C. We expected to find in
93 the F₁ hybrid progeny of this cross abundant potential in segregation for other important
94 viticultural traits, such as branching, angle of growth, leaf shape, root growth, periderm
95 formation, and disease resistance. We hypothesized, therefore, that their F₁ hybrid progeny
96 would allow for the mapping of economically relevant genomic loci.

97

98 **Materials and Methods**

99 *Mapping population.*

100 An F₁ mapping population was developed by crossing *V. rupestris* accession PI588160
101 (female parent) with *V. riparia* accession PI588271 (male parent) (Germplasm Resources
102 Information Network 2019) in 2014. Crosses were made in the field by manually removing
103 floral caps on the *V. rupestris* parent and applying dried collected pollen from the *V. riparia*
104 parent. Inflorescences were covered with paper bags for 3 weeks to prevent unintended
105 pollination. Seeds were collected from berries (fully colored and soft), vernalized for 4 weeks
106 at 4°C, and germinated under greenhouse conditions in a 1:1 mix of PRO-MIX and perlite. In
107 the spring of 2015, seedlings were planted in the vineyard nursery and grown without
108 irrigation or fertilizer, using pest management treatments as needed for powdery mildew,
109 downy mildew, black rot, phomopsis, and anthracnose. In 2018, the surviving seedlings (n =
110 257) were transplanted into a permanent research vineyard at the USDA clonal germplasm
111 repository in Geneva, NY (42.895208N, -77.009853W). An additional 100 seedlings were
112 germinated and maintained as potted plants at South Dakota State University as part of a
113 phenotyping project. The combined 357 vines were genotyped for the development of the
114 genetic maps.

115 116 *Genotyping.*

117 A young leaf was collected from each vine into a well of a 96-well plate and promptly frozen
118 and stored in a -80°C freezer until processing. Two grinder beads were then placed into each
119 tube and leaf tissue was ground using a Geno/Grinder 2000 (OPS Diagnostics LLC, Lebanon

120 NJ, USA). Genomic DNA was extracted from each F₁ progeny plant and parents with
121 DNeasy 96-well DNA extraction kits (Qiagen, Valencia CA, USA). Genotyping-by-
122 sequencing (GBS) was performed following the protocol design described by Elshire et al.
123 (2011) and modified by Hyma et al. (2015). Barcoded adapters were ligated for each
124 individual sample and single-end sequencing of 100 bp was performed using HiSeq 2000
125 (Illumina Inc., San Diego, CA, USA) at the Institute of Biotechnology, Genomics Facility,
126 Cornell University, Ithaca, NY. Illumina reads were submitted to the NCBI BioSample
127 Database (SAMN13512746 through SAMN13513110). The raw reads were demultiplexed,
128 parsed, trimmed for quality. Processed reads were aligned using BWA version 0.6.2-r126 (Li
129 and Durbin 2009) against the 12X.v2 *V. vinifera* PN40024 reference genome sequence
130 (RefSeq) (Jaillon et al. 2007, Canaguier et al. 2017). SNP genotypes were called using
131 TASSEL-GBS pipeline version 3.0.139 (Glaubitz et al. 2014).

132
133 *Marker generation and map construction.*

134 GBS reads that aligned to the *V. vinifera* RefSeq were screened for single nucleotide
135 polymorphisms (SNPs). The identified SNPs were filtered using VCFtools v0.1.13 (Danecek
136 et al. 2011) to retain only biallelic SNPs at a sequencing depth of ≥ 6 . Further, only SNPs
137 with missing genotypes of $\leq 20\%$ and with minor allele frequency of ≥ 0.2 were retained.
138 The resulting SNP data in the VCF file were then converted to JOINMAP®5.0 (Van
139 Ooijen 2006) format using NGSEP (Duitama et al. 2014). F₁ genotypes with more than 10%
140 missing SNP markers were discarded, and a goodness-of-fit (χ^2) test was performed to filter
141 out test-cross and intercross markers deviating from the 1:1 and 1:2:1 segregation ratio in the

142 progeny, respectively. Because segregation distortion is a natural phenomenon in outcrossing
143 species such as grape, markers showing a moderate degree of segregation distortion were
144 retained for the map construction and only significantly distorted markers ($p < 0.0005$) were
145 discarded. Identical markers were identified and removed from the analysis. Maternal and
146 paternal population nodes were created in JOINMAP 5.0 with marker types “lm × ll” and “nm
147 × np”, respectively, and parental maps were constructed following the two-way pseudo-test
148 cross approach (Grattapaglia and Sederoff 1994). Only 2nd round maps were accepted for
149 each parent, using the jump threshold of 5 (default), to maximize the number of markers
150 included in the maps while limiting the inclusion of markers with weak linkage. Markers of
151 “hk × hk” type were then used to integrate parental linkage maps into a consensus map. Each
152 linkage group was constructed with a threshold logarithm of odds (LOD) value of 14,
153 maximum recombination frequency of 0.4, and jump threshold of 5. Marker order was
154 determined with a regression mapping algorithm, and genetic distances were expressed in
155 Kosambi map units with parameters at default settings. Linkage maps were visualized
156 using the software LinkageMap View (Ouellette et al. 2017).

157
158 *Phenotyping the F₁ progeny for downy mildew resistance.*

159 In the greenhouse, phenotyping was carried out by quantifying downy mildew (DM)
160 resistance on naturally infected leaves of two replicate plants for each of 136 F₁ genotypes 5
161 days after the symptoms first appeared. Disease developed on naturally infected plants in the
162 greenhouse, was monitored during development and evaluated at a single time point when
163 shoots were at the 8-10 node stage. Scoring was performed using a disease resistance scale of

164 1 to 10, where 1 represented the highest susceptibility (100% of the leaves had more than
165 50% of the leaf area on the abaxial side covered with sporangiophores) and 10 the highest
166 resistance (all of the leaves had minimal or no sporangial growth). All leaves on a shoot were
167 used to provide the score (coverage over the entire shoot). Plants were then stripped and
168 pruned to 2 buds and sprayed with Dithane.

169
170 An *in vitro* disease assay was then performed to determine if the symptoms seen in the
171 greenhouse were reproducible under more tightly controlled conditions. The 86 individuals
172 phenotyped *in vitro* were part of the same F₁ population as those phenotyped following
173 natural infection, but only 20 individuals were shared between the two cohorts. Healthy
174 leaves from the third and fourth nodes from the apical meristem were surface sterilized in 1%
175 NaOCl solution for two minutes and then rinsed four times in sterile deionized water (dH₂O)
176 for five minutes per rinse. Four circular leaf disks, 2 cm in diameter, were excised from each
177 leaf and placed abaxial-side up on 0.8% water-agar plates in Petri dishes. Downy mildew was
178 collected from infected leaves in the greenhouse and propagated on susceptible leaves to
179 amplify the inoculum. A sporangial suspension of *P. viticola* was prepared by suspending
180 sporangia in dH₂O at a density of 70,000 sporangia/ml, which was then sprayed over the leaf
181 disks uniformly. Inoculated leaf disks were incubated overnight in darkness under axenic
182 conditions and transferred to a growth chamber with a temperature of 21 °C and a 5-hour/19-
183 hour dark/light diurnal cycle. The leaf disks were visually scored for disease resistance seven
184 days after inoculation. Leaf surface area coverage was estimated using OIV standard disease
185 resistance chart 452 (International Organization of Vine and Wine 2009), which uses a scale

186 of 1 to 9, where 1 and 9 represent the highest susceptibility and the highest resistance,
187 respectively (Supplemental Figure 1). Each leaf disk was evaluated by two observers
188 independently and their scores were averaged. Though the of scales of the greenhouse and *in*
189 *vitro* phenotyping had slightly different grading, they both had the same direction.

190 *Characterization of the downy mildew strain.*

191 To characterize the *P. viticola* strain responsible for this infection (named MO-1), the
192 genomic DNA of the pathogen was extracted by boiling sporangiophores in the presence of
193 5% Chelex, and a 235 bp-long internal transcribed spacer-1 (ITS-1) sequence of the 5.8S
194 ribosomal RNA gene was PCR-amplified using the ITS-1 primer pair specified by Rouxel et
195 al. (2014). The PCR product was then sequenced and aligned to the corresponding ITS
196 nucleotide sequence of other *P. viticola* cryptic species. To assess the virulence of MO-1 on
197 different grapevine species, the *in vitro* disease assay was performed using leaf disks of three
198 different grapevines, *V. riparia* Gloire de Montpellier, *M. rotundifolia* Thomas, and *V.*
199 *vinifera* F2-35, plus the parents of the F1 population. Leaf surface area coverage was
200 estimated using the 1-to-9 scale of the OIV standard disease resistance chart 452
201 (International Organization of Vine and Wine 2009),

202 203 *QTL analysis.*

204 QTL analysis was performed in MapQTL 6.0 (Van Ooijen 2009) using the integrated map.
205 The interval mapping (IM) method was applied to detect significant associations between
206 phenotypic traits and markers using a regression approach. Genome-wide LOD thresholds (p
207 < 0.05) were determined for each phenotype by performing 1000 permutations. The genetic

208 regions for significant LOD peaks were identified with corresponding 2-LOD intervals, the
209 predicted gene content in this region was identified using the most recent annotation of the
210 RefSeq (Grimplet et al. 2012, Canaguier et al. 2017), and the percentage of phenotypic
211 variance explained by each QTL was calculated. QTL graphs were generated in MapChart
212 version 2.32 (Voorrips 2002).

213 Results

214 *Linkage map construction.*

215 The removal of F₁ individuals with more than 10% missing data reduced the number of
216 individuals in the mapping population to 294. Filtering 348,888 SNPs across this population
217 for various quality parameters yielded 11,063 SNPs. Of the SNPs that satisfied the filtering
218 criteria, 3,436 SNPs were discarded because both parents were homozygous for these sites.
219 An additional 1,276 sites with unexpected genotypes were excluded from downstream
220 analysis. First, “lm × ll”- and “nn × np”-type SNP markers were used to construct parental
221 maps. Population nodes were created in JOINMAP®5.0 for each parent separately. An
222 additional 331 and 360 markers were removed from the maternal and paternal nodes,
223 respectively, because their segregation was distorted from the expected 1:1 ratio as
224 determined by χ^2 test ($p < 0.0005$). Upon the removal of identical markers from each parental
225 node, 1,462 and 1,351 female and male parent-informative markers following “nn × np” and
226 “ll × lm” segregation types were used for linkage map construction. For the female and male
227 parents, 1,177 and 1,115 significant markers (LOD threshold ≥ 14) were grouped into 19
228 different linkage groups covering 1,401.3 cM and 1,657.4 cM of genetic distance (Table 1),
229 respectively. Linkage groups were numbered according to the assignment of *V. vinifera*

230 RefSeq chromosome map-anchored SNP markers. For *V. rupestris*, the number of SNP
231 markers on each linkage group varied with a maximum of 114 on LG14 to a minimum of 31
232 on LG6. The longest and shortest linkage groups for *V. rupestris* were LG18 (108.7 cM) and
233 LG6 (58.6 cM), respectively. In *V. riparia*, LG7 and LG10 included maximum (92) and
234 minimum (33) number of SNP markers, respectively, and LG18 (125.1 cM) and LG9 (63
235 cM) were the longest and shortest linkage groups, respectively. Although the female map
236 contains a greater number of markers than the male map, it spans a shorter genetic length.
237 Furthermore, 291 “hk × hk”- type markers were combined with the male and female maps to
238 construct an integrated map. The integrated linkage map consists of 2,583 markers
239 distributed on 19 linkage groups and spans a genetic distance of 1,634.1 cM with an average
240 marker interval of 0.63 cM (Supplemental Figure 2). Synteny between marker genetic
241 positions on the linkage maps and their corresponding physical coordinates in the RefSeq are
242 shown in Supplemental Figure 3. The detailed genotype information for each marker across
243 294 F₁ progeny are shown in Supplemental Tables 1, 2, and 3 for the *V. rupestris*, the *V.*
244 *riparia*, and the integrated map, respectively. Parental map quality was then further tested
245 using R/qtl (Broman et al. 2003, script provided in Supplemental File 1). Pairwise
246 recombination fractions demonstrated tight linkage within, but not across, different linkage
247 groups (Supplemental Figure 4).

248
249 *QTL mapping of the sex-determining locus.*

250 To verify the correctness of the linkage maps, pistillate/staminate flower data were used to
251 perform interval mapping to map the sex-determining locus. Of 203 flower-bearing F₁

252 individuals, 101 had pistillate, 102 had staminate, and none had hermaphroditic flowers,
253 indicating that the female parent was homozygous for the recessive female allele and the
254 male parent was heterozygous for the dominant male allele. A single major QTL was
255 detected at a genetic position of 21.99 cM on chromosome 2 (chr2) in the integrated map
256 with a peak LOD score of 60.32 (Supplemental Figure 5). This QTL (QTL.Sex) explained
257 80.7% of the phenotypic variance, and its localization to chr2 is in agreement with earlier
258 reports (Dalbó et al. 2000, Riaz et al. 2006, Marguerit et al. 2009).

259
260 *Characterization of the DM pathogen.*

261 The nucleotide sequence of the ITS-1 fragment amplified from the DM strain was identical to
262 the corresponding fragment of Clade-A of the *P. viticola* species complex (Supplemental
263 Figure 6), which established it as a member of the riparia cryptic species of *P. viticola*.
264 (Rouxel et al. 2014). To characterize the virulence of the MO-1 strain, it was used to
265 inoculate three different grapevines, *V. riparia* Gloire de Montpellier, *M. rotundifolia*
266 Thomas, and *V. vinifera* F2-35. *M. rotundifolia* Thomas appeared immune to the strain, *V.*
267 *riparia* Gloire de Montpellier proved partially resistant, while *V. vinifera* F2-35 was highly
268 susceptible (Fig. 1), indicating that the strain represents an aggressive pathogen of cultivated
269 grapes. Both parents of the F₁ progeny had higher levels of resistance to MO-1 than *V.*
270 *vinifera* (Fig. 1). While, based on its phenotypic appearance, we consider the downy mildew
271 population used in this study to be a single strain, we have not propagated it from a single
272 sporangium to ensure that inoculations were done with a pure culture.

273
274

275 *QTL mapping of DM resistance.*

276 Segregation of the DM resistance phenotype in the F₁ progeny suggested that this trait was
277 quantitative and determined by multiple loci (Supplemental Figure 7). Of the 20 individuals
278 that were present in both the naturally and *in vitro*-infected cohorts, 16 had similarly
279 moderate resistance ratings under both conditions. The four that substantially differed in DM
280 coverage were all rated as highly susceptible (1 on a 1-to-10 point scale) in response to
281 natural infection, but moderately resistant under *in vitro* conditions. Analysis of resistance
282 levels in naturally infected vines led to the detection of a major QTL at a genetic position of
283 12.46 cM on chr10 in the integrated map (Rpv28.1, Fig. 2). This QTL, which independently
284 mapped to the female parent but not to the male parent, had an LOD value of 32.32, and
285 explained 66.5% of the phenotypic variance for disease resistance. QTL analysis of
286 resistance levels in *in vitro*-inoculated leaf disks led to similar results: a significant QTL for
287 resistance was detected at a genetic position of 15.09 cM on chr10 on the integrated map
288 explaining 24.3% of the phenotypic variance (Rpv28.2, Fig. 2; mean and standard deviation
289 scores for each genotype are reported in Supplemental Table 4). The *in vitro*-mapped QTL
290 encompassed the entire Rpv28.1 interval. GBS markers that fall within the 2-LOD interval of
291 Rpv28.1 and Rpv28.2, their LOD scores and their projected position in the 12X.v3 assembly
292 of *V. vinifera* (Canaguier et al. 2017) are listed in Supplemental Table 5. The 2-LOD
293 interval surrounding Rpv28.2 is delimited by the GBS markers S10_419927 and
294 S10_3959571, which correspond to the physical interval of chr10:419,927..3,959,571.
295 Predicted genes within Rpv28.1 as projected to the *V. vinifera* 12X.v3 reference genome
296 sequence are listed in Supplemental Table 6. No significant QTL for resistance was detected

297 in the *V. riparia* parent under natural or *in vitro* conditions. Results of QTL analyses are
298 summarized in Table 2; effect plots are shown in Fig. 3.

299 Discussion

300 The American grape species *V. rupestris* and *V. riparia* have adapted to disparate
301 environmental conditions and occupy different but overlapping geographic ranges (Callen et
302 al. 2016). They also evolved to have contrasting characteristics in dormancy, morphology,
303 and growth habits (Munson 1909). Exploration of the genetic basis of their environmental
304 adaptation is warranted because the viticulture industry is in need of genetic resources to
305 mitigate the environmental impact of global climate change. The economic value of these
306 species is evidenced by their status as cornerstone resources for the development of disease-
307 resistant, phylloxera- and stress-tolerant, fruit-bearing and rootstock cultivars during the past
308 one and a half centuries (Reisch et al. 2012). Despite their proven value, *V. rupestris* and *V.*
309 *riparia* have yet to be explored for their vast genetic diversity across North America. *V.*
310 *rupestris* has been under pressure due to habitat loss and is threatened by genetic erosion
311 (Pap et al. 2015). These conditions add urgency to a broader examination of its native
312 populations. In a recent study, Klein et al. (2018) used GBS markers to examine the genetic
313 diversity of 27 *V. rupestris* and 80 *V. riparia* accessions housed at the USDA-ARS Grape
314 Germplasm Collection. While their data are limited to the accessions maintained in the
315 repository, their work has set the technological and phylogenetic foundations for a broader
316 exploration of the natural populations of these and other wild grape relatives (Klein et al.
317 2018).

318 We report here the construction of genetic linkage maps for *V. rupestris* and *V.*
319 *riparia* based on an F₁ population produced from a cross between these two species. In terms
320 of marker position, the genomes of both parents had a high degree of synteny with the
321 genome of *V. vinifera*. (Supplemental Figure 3). We observed that *V. rupestris* and *V. riparia*
322 had only 9.94% and 8.87% of their markers assigned to a linkage group that was different
323 from the *V. vinifera* RefSeq linkage group assignment (Supplemental Figure 2). Gardner et
324 al. (2014) and Antanaviciute et al. (2012) also reported similarly conflicting results between
325 genetic and RefSeq positions for 18.3% and 13.7% SNP markers in apple. Such
326 disagreements between linkage maps and RefSeqs do not necessarily indicate mapping
327 errors, but may result from the presence of paralogous genomic regions or incorrect RefSeq
328 sequence assembly. By performing a map validation step using the flower sex phenotype, we
329 were able to verify the linkage maps we generated, since the genomic position of the sex
330 locus was already known. This gave us confidence in the accuracy of our map and the ability
331 to reproduce the mapping of a well-known locus with our set of markers, placed as they are
332 on the genetic maps.

333 Defense-related genes tend to be in the heterozygous state in plants (McDowell and
334 Simon 2006), and genes that confer resistance to the same pathogen are often located at
335 different loci in various grape genotypes (Gadoury et al. 2012, Buonassisi et al. 2017).
336 Consequently, two resistant grapevine parents will likely produce an F₁ population in which
337 defense related traits will segregate, as recently demonstrated by Divilov et al. (2018). We
338 followed a similar approach as described by Divilov et al. (2018) in that we established an F₁
339 hybrid population from a cross between two DM-resistant accessions. DM resistance

340 segregated in the F₁ progeny, which enabled us to map a major QTL (LOD of 32.32),
341 Rpv28.1, in the female parent accounting for 66.5% of the phenotypic variance in naturally
342 infected plants under greenhouse conditions. Repeating this analysis using a leaf disk DM
343 inoculation assay led to mapping of a resistance QTL, Rpv28.2 (also from the female parent),
344 which overlaps with Rpv28.1 confirming the contribution of this locus to defense against
345 DM. This QTL, however, explained only 24.3% of the phenotypic variance and had an LOD
346 value of 5.2, indicating that the trait is strongly influenced by the environment. Other
347 possible reasons for the lower LOD value with respect to the QTL detected in the greenhouse
348 assay might include limited population size and/or phenotyping errors. Notably, of the 20
349 vines shared between the naturally infected and the *in vitro*-inoculated cohorts, 16 had
350 similar and 4 had different phenotypes. All four of the latter were rated as highly susceptible
351 in the greenhouse, but moderately resistant *in vitro*. Unfortunately, the number of plants is
352 too low to address the question as to why these four had so much lower resistance in the
353 greenhouse. No QTL were identified from the male parent, which is surprising given the
354 results of our virulence assay on multiple species (Figure 1), in which the *V. riparia* parent
355 showed an even higher level of resistance to this DM strain than the *V. rupestris* parent. One
356 possible reason for this finding may be the presence of multiple components of resistance
357 that contribute at low levels to the observed resistance phenotype in the male parent, which
358 were below the threshold of detection in the offspring. Other possibilities include a major
359 QTL that was present in a homozygous state or a in region of the genome with low marker
360 coverage. We report here the identification of two overlapping DM resistance loci, Rpv28.1
361 and Rpv28.2. While these may in fact represent one single resistance locus, we identify them

362 in separate assays that produced different LOD scores, different levels of variance explained,
363 and different numbers of markers included under the peaks. Therefore, we think it more
364 prudent to maintain separate nomenclature for these loci.

365 While the high LOD value for Rpv28.1 and its reproducibility lend strong support for
366 the presence of a resistance QTL on chr10, our experiments have limitations. Importantly,
367 resistance was likely assessed against a single strain of *P. viticola*. Furthermore, our results
368 lack multi-season field data. At the time of writing, the entire F₁ population has been
369 established in the field in both New York and Missouri. Both locations are known for high
370 DM disease pressure, but represent different climates where the prevailing DM populations
371 are likely dominated by different cryptic species of *P. viticola* (Rouxel et al. 2014). In the
372 future, it will be important to test the resistance of this progeny under vineyard
373 conditions. The New York and Missouri plantings will enable us to collect data on how
374 various *P. viticola* strains and climatic conditions influence the performance of this QTL in
375 the field.

376 Rpv28.1 is responsible for 66.5% of resistance against an aggressive DM pathogen
377 and, therefore, it may be utilized for breeding grape cultivars with reduced requirement for
378 fungicide input. The applicability of this locus is all the more relevant because, to our
379 knowledge, it is the first defense-related QTL in this region of chr10. Previously, Kortekamp
380 et al. (2008) hypothesized on the basis of gene expression measurements that DM resistance
381 in the hybrid cultivar Regent was encoded by three CC-NBS-LRR-type resistance genes on
382 chr10. These genes mapped, however, at a physical distance of at least 13 Mb away from
383 Rpv28.1 and Rpv28.2 near the end of the opposite arm of chr10. Interestingly, the DM-

384 resistant parent, *V. rupestris* B38, was identified by Divilov et al (2018) to harbor another
385 QTL for DM resistance on a different chromosome from the QTL identified in our study
386 (Rpv19 on chr14). We did not detect any QTL for DM resistance at this locus in neither the
387 greenhouse assay nor the *in vitro* assay performed in this study. The most likely reason that
388 we did not observe this QTL is that the DM isolate in this study was different from the isolate
389 that elicits disease resistance conveyed by Rpv19. Additionally, Rpv19 resistance is
390 characterized by a hypersensitive reaction that was not observed in the Rpv28 resistance
391 phenotype. Therefore, *V. rupestris* B38 is a promising source for multiple resistance loci and
392 may prove to be a useful component of “gene pyramiding” schemes. The premise of gene
393 pyramiding is that combining various defense mechanisms against the same class of
394 pathogen will result in more stable resistance than the introgression of a single resistance
395 gene, particularly when considering the ability of different resistance gene products to
396 recognize different pathogen isolates. Based on insight into the evolution of R gene in several
397 plant species (McDowell and Simon, 2006), it is not surprising that *V. rupestris* B38 several
398 resistance factors against the same pathogen. The combination of potentially multiple
399 resistance mechanisms represented by Rpv19 and Rpv28, afford protection against different
400 isolates of the pathogen and provide a survival advantage in nature. Future work will assess
401 the virulence of other DM isolates from different *P. viticola* clades on Rpv28 DM resistant
402 individuals to ascertain the breadth of recognition for this locus.

403 Introgression of several loci to provide resistance against the same pathogen is only
404 possible with marker-assisted selection (MAS). The GBS markers that define the new QTL
405 may prove valuable for the development of molecular markers for MAS (Table 2 and

406 Supplemental Table 5). Myles et al. (2010) found that only 24.3% of the SNPs segregated
407 within both *V. vinifera* and wild *Vitis* germplasm, suggesting that a portion of the
408 heterozygous *V. rupestris* GBS markers can be readily selected when this resistance
409 haplotype is introgressed into a predominantly *V. vinifera* background. Although SNP-based
410 genotyping has been gaining popularity in grape breeding, many breeding programs still rely
411 on simple sequence repeat (SSR) markers. A significant number of SSR markers have been
412 shown to be transferable from *V. vinifera* to wild *Vitis* species and hybrid grapes (Pap et al.
413 2015, Hammer et al. 2017, Garris et al. 2009). We have identified six SSR markers that fall
414 within or closely flank the region spanning Rpv28.1 and Rpv28.2 (Supplemental Table 7).
415 These markers were originally developed for *V. vinifera*, and their applicability and
416 polymorphism in *V. rupestris* B38 remains to be tested. Given that *V. rupestris* B38 is now
417 known to harbor multiple DM resistance genes (Rpv19 and Rpv28), marker assisted selection
418 will be essential to identifying which resistance alleles are passed on to its progeny.

419 Highly effective MAS, however, will require the development of markers closely-
420 linked to Rpv28.1. The strong synteny (Supplemental Figure 3) and partial conservation of
421 SSR markers between *V. vinifera* and *V. rupestris* indicate that designing SSR primers based
422 on the orthologous *V. vinifera* sequences may be a workable, though potentially ineffective,
423 way to achieve this goal. A genomic library or a genome assembly of *V. rupestris* would
424 make this approach more fruitful. Other marker types, including rhAmpSeq and KASP could
425 also be useful for this purpose and for further mapping work with this population. In
426 addition, it may prove useful for future breeding efforts to survey the extant grapevine
427 germplasm repositories for the markers associated with Rpv28 resistance, and assess allelic

428 diversity at this locus. Considering the importance of this species as a resource for grape
429 breeding, the establishment of genomic tools would be a well-justified investment for the
430 grape research community.

431 Conclusion

432 The hypothesis that a *V. rupestris* × *V. riparia* F1 progeny can facilitate the mapping of
433 economically relevant loci was supported by the identification of the DM resistance QTL
434 *Rpv28.1* and *Rpv28.2* in the *V. rupestris* genome. The novelty of this resistance locus
435 suggests that the biological diversity of North American *Vitis* remains an extensive and still
436 largely unexplored resource for grapevine breeding. In addition, this paper, including the
437 supplementary material, provides a valuable resource for grape breeders and geneticists, as
438 well as for teaching genetic mapping in an outcrossing species.

439 Literature Cited

- 440 Agurto M, Schlechter RO, Armijo G, Solano E, Serrano C, Contreras RA, Zúñiga GE and
441 Arce-Johnson P. 2017. RUN1 and REN1 pyramiding in grapevine (*Vitis vinifera* cv. crimson
442 seedless) displays an improved defense response leading to enhanced resistance to powdery
443 mildew (*Erysiphe necator*). *Front Plant Sci* 8:758.
444
- 445 Alleweldt G and Possingham JV. 1988. Progress in grapevine breeding. *Theor Appl Genet*
446 75:669–673.
447
- 448 Antanaviciute L, Fernández-Fernández F, Jansen J, Banchi E, Evans KM, Viola R, Velasco
449 R, Dunwell JM, Troggio M and Sargent DJ. (2012) Development of a dense SNP-based
450 linkage map of an apple rootstock progeny using the *Malus* Infinium whole genome
451 genotyping array. *BMC Genomics* 13:203.
452
- 453 Broman KW, Wu H, Sen S and Churchill GA. 2003. R/qtl: QTL mapping in experimental
454 crosses. *Bioinformatics* 19:889–890.
455

- 456 Buonassisi D, Colombo M, Migliaro D, Dolzani C, Peressotti E, Mizzotti C, Velasco R,
457 Masiero S, Perazzolli M and Vezzulli S. 2017. Breeding for grapevine downy mildew
458 resistance: a review of “omics” approaches. *Euphytica* 213:103.
459
- 460 Callen ST, Klein LL and Miller AJ. 2016. Climatic niche characterization of 13 North
461 American *Vitis* species. *Am J Enol Vitic* 67:339–349.
462
- 463 Canaguier A, et al. 2017. A new version of the grapevine reference genome assembly
464 (12X.v2) and of its annotation (VCost.v3). *Genom Data* 14:56–62.
465
- 466 Dalbó MA, Ye GN, Weeden NF, Steinkellner H, Sefc KM and Reisch BI. 2000. A gene
467 controlling sex in grapevines placed on a molecular marker-based genetic map. *Genome*
468 43:333–340.
469
- 470 Danecek P, et al. 2011. The variant call format and VCFtools. *Bioinformatics* 27:2156–
471 2158.
472
- 473 Di Gaspero G, et al. 2012. Selective sweep at the *Rpv3* locus during grapevine breeding for
474 downy mildew resistance. *Theor Appl Genet* 124:277–286.
475
- 476 Divilov K, Barba P, Cadle-Davidson L and Reisch B. 2018. Single and multiple phenotype
477 QTL analyses of downy mildew resistance in interspecific grapevines. *Theor Appl Genet*
478 131:1133–1143.
479
- 480 Duitama J, Quintero JC, Cruz DF, Quintero C, Hubmann G, Foulquié-Moreno MR,
481 Verstrepen KJ, Thevelein JM and Tohme J. 2014. An integrated framework for discovery
482 and genotyping of genomic variants from high-throughput sequencing experiments. *Nucleic*
483 *Acids Res* 42:6.
484
- 485 Elshire RJ, Glaubitz JC, Sun Q, Poland JA, Kawamoto K, Buckler ES and Mitchell SE. 2011.
486 A robust, simple genotyping-by-sequencing (GBS) approach for high diversity species.
487 *PLOS One* 6:e19379.
488
- 489 Feechan A, et al. 2013. Genetic dissection of a TIR-NB-LRR locus from the wild North
490 American grapevine species *Muscadinia rotundifolia* identifies paralogous genes conferring
491 resistance to major fungal and oomycete pathogens in cultivated grapevine. *Plant J* 76:661–
492 674.
493
- 494 Gadoury DM, Cadle-Davidson L, Wilcox WF, Dry IB, Seem RC and Milgroom MG. 2012.
495 Grapevine powdery mildew (*Erysiphe necator*): a fascinating system for the study of the
496 biology, ecology and epidemiology of an obligate biotroph. *Molecular Plant Pathol* 13:1–16.
497

- 498 Gardner KM, Brown P, Cooke TF, Cann S, Costa F, Bustamante C, Velasco R, Troglio M
499 and Myles S. 2014. Fast and Cost-Effective Genetic Mapping in Apple Using Next-
500 Generation Sequencing. *G3* (Bethesda) 4:1681–1687.
501
- 502 Garris, A, Clark, L, Owens, C, Luby, J, McKay, S, Mathiason, K and Fennell, A (2009)
503 Mapping of photoperiod-induced growth cessation in the wild grape *Vitis riparia*. *J.*
504 *American Society of Horticulture Science* 134:261–272.
505
- 506 Germplasm Resources Information Network [Internet]. Beltsville (MD): United States
507 Department of Agriculture, Agricultural Research Service. November 28, 2019. Available
508 from: <http://www.ars-grin.gov/>.
509
- 510 Glaubitz JC, Casstevens TM, Lu F, Harriman J, Elshire RJ, Sun Q and Buckler ES. 2014.
511 TASSEL-GBS: a high capacity genotyping by sequencing analysis pipeline. *PLoS One*
512 9:e90346.
513
- 514 Grattapaglia D and Sederoff R. 1994. Genetic linkage maps of *Eucalyptus grandis* and
515 *Eucalyptus urophylla* using a pseudo-testcross: Mapping strategy and RAPD markers.
516 *Genetics* 137:1121–1137.
517
- 518 Grimplet J, VanHemert J, Carbonell-Bejerano P, Diaz-Riquelme J, Dickerson J, Fennell A,
519 Pezzotti M and Martinez-Zapater JM. 2012. Comparative analysis of grapevine whole-
520 genome gene predictions, functional annotation, categorization and integration of the
521 predicted gene sequences. *BMC Research Notes* 5:213–222.
522
- 523 Hyma KE, Barba P, Wang M, Londo JP, Acharya CB, Mitchell SE, Sun Q, Reisch B and
524 Cadle-Davidson L. 2015. Heterozygous mapping strategy (HetMappS) for high resolution
525 genotyping-by-sequencing markers: A case study in grapevine. *PLoS One* 10:8.
526
- 527 International Organization of Vine and Wine. 2009. Technical Standards and
528 Documents. (2nd ed.). Organisation Internationale de la Vigne et du Vin Paris, France.
529
- 530 Jaillon O, et al. 2007. The grapevine genome sequence suggests ancestral hexaploidization in
531 major angiosperm phyla. *Nature* 449:463–467.
532
- 533 Klein LL, Miller AJ, Ciotir C, Hyma K, Uribe-Convers S and Londo J. 2018. High-
534 throughput sequencing data clarify evolutionary relationships among North American *Vitis*
535 species and improve identification in USDA *Vitis* germplasm collections. *Am J Botany*
536 105:215–226.
537
- 538 Kortekamp A, Welter L, Vogt S, Knoll A, Schwander F, Töpfer R and Zyprian E. 2008.
539 Identification, isolation and characterization of a CC-NBS-LRR candidate disease resistance
540 gene family in grapevine. *Mol Breeding* 22:421–432.

- 541
542 Li H and Durbin R. 2009. Fast and accurate short read alignment with Burrows–Wheeler
543 transform. *Bioinformatics* 25:1754–1760.
544
- 545 Liang Z, et al. 2019. Whole-genome resequencing of 472 *Vitis* accessions for grapevine
546 diversity and demographic history analyses. *Nat Commun* 10:1190.
547
- 548 Marguerit E, Boury C, Manicki A, Donnart M, Butterlin G, Némorin A, Wiedemann-
549 Merdinoglu S, Merdinoglu D, Ollat N and Decroocq S. 2009. Genetic dissection of sex
550 determinism, inflorescence morphology and downy mildew resistance in grapevine. *Theor*
551 *Appl Genet* 118:1261–1278.
552
- 553 McDowell JM and Simon SA. 2006. Recent insights into R gene evolution. *Mol Plant Pathol*
554 7:437-448.
- 555 Migicovsky Z, et al. 2016. Genomic ancestry estimation quantifies use of wild species in
556 grape breeding. *BMC Genomics* 17:478.
557
- 558 Munson TV. 1909. *Foundations of American Grape Culture*. Munson TV and Son, Texas.
559
- 560 Myles S, Chia J-M, Hurwitz B, Simon C, Zhong GY, Buckler E and Ware D. 2010. Rapid
561 genomic characterization of the genus *Vitis*. *PLoS One* 5:e8219.
562
- 563 Ouellette LA, Reid RW, Blanchard SG, and Brouwer CR. 2017. LinkageMapView—
564 rendering high-resolution linkage and QTL maps. *Bioinformatics* 34:306–307.
565
- 566 Pap D, Miller AJ, Londo JP, and Kovács LG. 2015. Population structure of *Vitis rupestris*, an
567 important resource for viticulture. *Am J Enol Vitic* 66:403–410.
568
- 569 Reisch BI, Owens CL and Cousins PS. 2012. Grape. In: Badenes M, Byrne D (eds) *Fruit*
570 *Breeding*. Handbook of Plant Breeding, vol 8. Springer, Boston, MA, pp 225–262.
571
- 572 Riaz S, Krivanek AF, Xu K and Walker MA. 2006. Refined mapping of the Pierce's disease
573 resistance locus, PdR1, and Sex on an extended genetic map of *Vitis rupestris* × *V. arizonica*.
574 *Theor Appl Genet* 113:1317–29.
575
- 576 Riaz S, Pap D, Uretsky J, Laucou V, Boursiquot J-M, Kocsis L and Walker AM. 2019.
577 Genetic diversity and parentage analysis of grape rootstocks. *Theor Appl Genet* 132:1847–
578 1860.
579
- 580 Rouxel M, et al. 2014. Geographic distribution of cryptic species of *Plasmopara viticola*
581 causing downy mildew on wild and cultivated grape in eastern North America.
582 *Phytopathology* 104:692–701.
583

- 584 Vannozzi A, Dry IB, Fasoli M, Zenoni S and Lucchin M. 2012. Genome-wide analysis of the
585 grapevine stilbene synthase multigenic family: genomic organization and expression profiles
586 upon biotic and abiotic stresses. *BMC Plant Biol* 12:130.
587
- 588 Van Ooijen JW. 2006. JoinMap® 5, Software for the calculation of genetic linkage maps in
589 experimental populations of diploid species. Kyazma B.V., Wageningen, The Netherlands.
590
- 591 Van Ooijen, JW. 2009. MapQTL®6, Software for the mapping of quantitative trait loci in
592 experimental populations of diploid species. Kyazma B.V., Wageningen, Netherlands.
593
- 594 Voorrips, RE. 2002. MapChart: Software for the graphical presentation of linkage maps and
595 QTLs. *The Journal of Heredity* 93:77–78.
596
- 597

Table 1 Distribution of SNP markers and the total genetic length in Kosambi distance across the *V. rupestris* B38 and *V. riparia* HP-1 parental and integrated maps.

Linkage group	Number of markers			Size (cM)			Average distance between markers (cM)		
	<i>V. rupestris</i> map	<i>V. riparia</i> map	Integrated map	<i>V. rupestris</i> map	<i>V. riparia</i> map	Integrated map	<i>V. rupestris</i> map	<i>V. riparia</i> map	Integrated map
LG1	42	64	125	80.5	94.8	96.0	0.52	0.68	0.77
LG2	50	43	99	64.5	77	75.2	0.78	0.56	0.76
LG3	51	57	115	65.4	75.7	77.3	0.78	0.75	0.67
LG4	61	64	139	71	88.9	87	0.86	0.72	0.63
LG5	63	59	139	71.8	83.5	82.4	0.88	0.71	0.59
LG6	31	53	94	58.6	86.8	85	0.53	0.61	0.90
LG7	98	92	209	95.9	116.7	114.6	1.02	0.79	0.55
LG8	57	50	119	75.7	89.8	88	0.75	0.56	0.74
LG9	66	37	110	63.2	63	67.8	1.04	0.59	0.62
LG10	65	33	107	65.8	80.9	74.8	0.99	0.41	0.70
LG11	42	39	90	65.2	75.2	74.4	0.64	0.52	0.83
LG12	68	71	163	87.6	74.3	90.9	0.78	0.96	0.56
LG13	48	80	159	80	98.3	96.5	0.60	0.81	0.61
LG14	110	86	228	88.4	96.4	93.9	1.24	0.89	0.41
LG15	55	54	117	65.6	95.7	93.3	0.84	0.56	0.80
LG16	78	49	143	66.3	82.1	74.5	1.18	0.60	0.52
LG17	41	53	102	64.4	72.7	71.6	0.64	0.73	0.70
LG18	78	74	172	108.7	125.1	115.3	0.72	0.59	0.67
LG19	73	57	153	62.7	80.5	75.6	1.16	0.71	0.49
Total	1177	1115	2583	1401.3	1657.4	1634.1	0.84	0.67	0.63

Table 2 Summary of QTL analysis results performed in the F1 hybrid progeny of *V. rupestris* B38 and *V. riparia* HP-1.

Trait	Parent of origin	Peak position (cM)	^a Interval (cM)	Nearest marker	LOD	^b LOD threshold	^c Explained variance (%)	^d Flanking markers
Sex	<i>V. riparia</i>	21.99	21.85-22.2	S2_4599939	60.32	4.8	80.7	S2_3835305, S2_4650244
DM resistance (<i>in vitro</i>)	<i>V. rupestris</i>	15.098	1.8-19.8	S10_3024940	5.20	4.8	24.3	S17_17189505, S10_2674703
DM resistance (in greenhouse)	<i>V. rupestris</i>	12.456	11.86- 14.85	S10_1285522	32.32	4.8	66.5	S10_2470297, S10_2868961

^a2-LOD interval on the integrated genetic map.

^bGenome-wide LOD threshold obtained with 1000 permutations at $p = 0.05$.

^cPercentage of phenotypic variance explained by QTL.

^dMarkers on each side of the largest LOD peak.

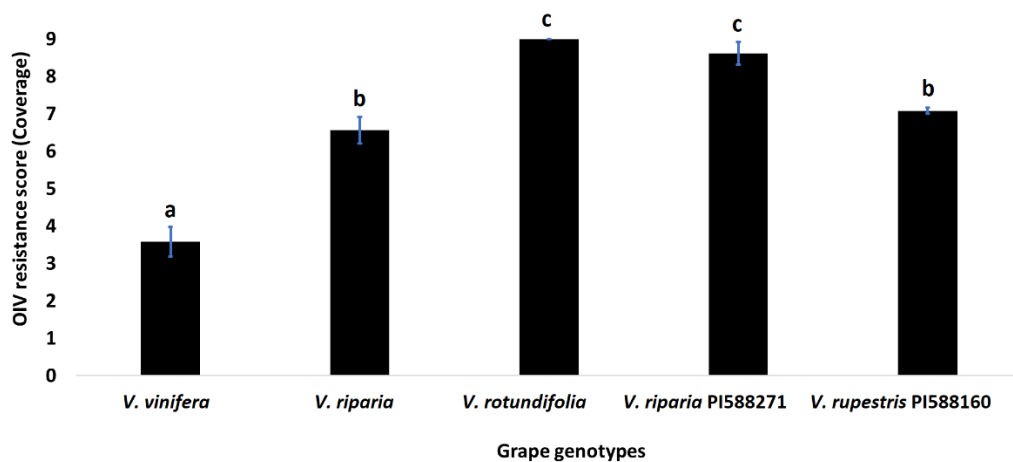


Figure 1 Resistance to *P. viticola* strain MO-1 in five grapevine genotypes. Level of resistance was measured as leaf area covered by sporangiophores following OIV standards in *V. vinifera* F2-35, *V. riparia* Gloire de Montpellier, and *M. rotundifolia* Thomas, and parent genotypes *V. riparia* HP-1 (PI588271), and *V. rupestris* B38 (PI588160).

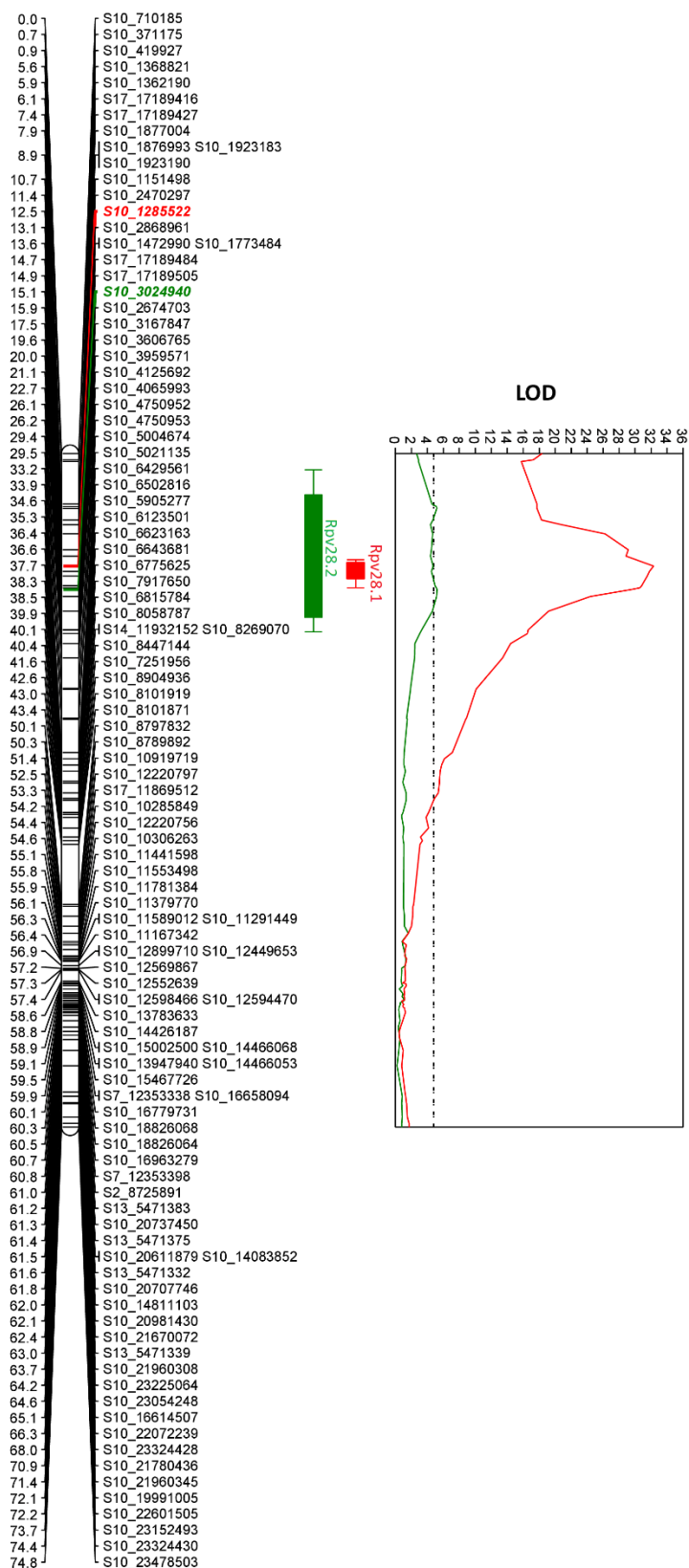


Figure 2 QTL analysis of downy mildew resistance across linkage group 10. The left panel represents the linkage map for LG 10 with marker ID and corresponding genetic position (cM). The right panel shows the LOD scores obtained from interval mapping for downy mildew resistance (red: greenhouse inoculation and green: *in vitro* inoculation) for each marker in the integrated genetic map. The solid boundary of red and green box plots, and extreme boundary represented by their whiskers indicate 1- and 2-LOD intervals for Rpv28.1 and Rpv28.2, respectively. The horizontal black dashed-dotted line represents genome-wide LOD threshold (1000 permutations) at a 5% level of significance. Markers in red and green color on the map represent markers with the largest LOD value.

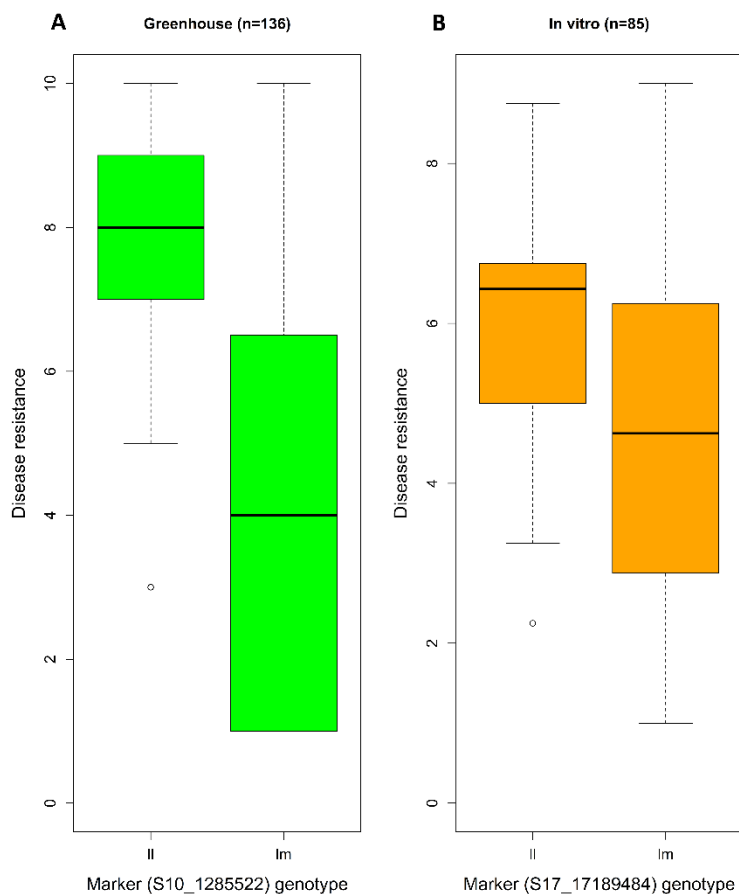


Figure 3 Effect plots showing the relative contribution to downy mildew resistance of QTL Rpv28.1 (S10_1285522) and Rpv28.2 (S17_17189484) in homozygous and heterozygous state.